J. S. Afr. Inst. Min. Metall., vol. 92, no.7.
Jul. 1992. pp.195-214.

Rigorously determined support characteristics and support-design method for tunnels subject to squeezing conditions

by H.A.D. Kirsten* and P.J. Bartlett†

SYNOPSIS

A two-dimensional numerical scheme for the simulation of the plastic stress–strain properties of rock, and the various components of rock reinforcement and shotcrete, was used to rigorously determine the characteristics of tunnel support under squeezing conditions. D-shaped tunnels varying in size from 2,8 to 6,5 m in height and width were considered. The four main mining stages in the BA5 block cave on Premier Mine were simulated as alternative sets of field stresses. The rock reinforcement comprised 1,8 m long fully grouted rockbolts and 6,0 m long fully grouted cable anchors at various spacings, and of various tensile and bond strengths. Various thicknesses of shotcrete and footwall support configurations were also considered.

It was found that shotcrete and rock reinforcement, owing to inherent differences in stiffness, do not function in unison. As monolithic application, shotcrete has an overriding avidity for the imposed loading and destructs itself unless of extraordinary thickness. Under squeezing conditions, it accordingly supports the excavation surface while the rock reinforcement contains on-going convergence. The loads in the various support components can be determined only by simulation of the shotcrete as a stress-relieved medium to represent its broken condition in the field.

The loads in the rock reinforcement vary around a tunnel and are the largest in the sidewalls. The loads increase with an increase in tunnel dimensions, the increase in load in the sidewall due to an increase in height being larger than that in the hanging- and footwalls due to an increase in width. Depending on the strength of the rock, the loads in the rock reinforcement become prohibitively large beyond a certain size of tunnel.

The reinforcement of footwall rock can be omitted without adversely affecting that in other walls, provided the tensile and bond strengths of the reinforcement are not limited. The resulting footwall heave may, however, result in undermining of the reinforcement in the adjoining walls. A relative depth of anchor of 1,37 provides adequate bond strength in the larger sizes of tunnel, whereas, in smaller tunnels, anchor length is determined by the allowable convergence.

The lack of full column grouting adversely affects the efficiency of rock reinforcement to a major extent. The loads in rock reinforcement are very sensitive to the strength of the rock. Owing to a lack in refinement and calculational rigour, empirical classification systems are an inappropriate means for the design of tunnel support in squeezing conditions and, as a result, grossly under-estimate the support requirements.

SAMEVATTING

'n Tweedimensionele numeriese skema vir die simulering van die plastiese spanning-vervormingseienskappe van rots en die verskillende bestanddele van rotsversterking en spuitbeton is gebruik vir die nougesette bepaling van die eienskappe van tonnelbestutting in druktoestande. D-vormige tonnels wat wissel van 2,8 tot 6,5 m in hoogte en breedte is in oënskou geneem. Die vier hoofmynboustadiums in die grot in blok BA5 by Premiermyn is as alternatiewe stelle veldspannings gesimuleer. Die rotsversterking het bestaan uit ten volle vasgebryde rotsboute met 'n lengte van 1,8 m, en ten volle vasgebryde kabelankers met 'n lengte van 6,0 m, op verskillende afstande en met verskillende trek- en verbandsterktes. Verskillende diktes spuitbeton en vloerstutkonfigurasies is ook in oënskou geneem.

Daar is gevind dat spuitbeton en rotsversterking vanweë inherente verskille in styfheid nie in harmonie funksioneer nie. As 'n monolitiese aanwending het spuitbeton 'n oorheersende gierigheid vir die opgelegde belasting en vernietig homself tensy dit buitengewoon dik is. Onder druktoestande ondersteun dit dus die oppervlak van die uitgrawing terwyl die rotsversterking voortgesette konvergensie bevat. Die laste in die verskillende dele van die bestutting kan slegs bepaal word deur die simulasie van die spuitbeton as 'n ontspande medium om sy gebroke toestand in die veld voor te stel.

Die laste in die rotsversterking wissel om 'n tonnel en is die grootste in die sywande. Die laste neem toe met 'n toename in die afmetings van die tonnel, en die toename in die belasting in die sywand as gevolg van 'n toename in hoogte is groter as die in die dakke en vloere as gevolg van 'n toename in breedte. Afhangende van die laste in die rotsversterking, word die laste onmoontlik groot bo 'n sekere tonnelgrootte.

Die versterking van die vloerrots kan weggelaat word sonder om dié in die ander wande nadelig te beïnvloed mits die trek- en verbandsterkte van die versterking nie aan bande gelê word nie. Die gevolglike sysing van die vloer kan egter lei tot die ondermyning van die versterking in die aangrensende wande. 'n Relatiewe ankerdiepte van 1,37 verskaf toereikende verbandsterkte in groter tonnels terwyl die ankerlengte in kleiner tonnels deur die toelaatbare konvergensie bepaal word.

Die gebrek aan die volledige vasbrying van kolomme het 'n baie belangrike nadelige uitwerking op die doeltreffendheid van die rotsversterking. Die laste in die rotsversterking is baie sensitief vir die sterkte van die rots. Vanweë 'n gebrek aan verfyning en nougesetheid met die berekenings is empiriese klassifikasiestelsels 'n ongeskikte metode vir die ontwerp van tonnelbestutting in druktoestande en lei gevolglik tot 'n gruwwe onderskatting van die stutvereistes.

* Steffen, Robertson & Kirsten Inc., P.O. Box 55291, Northlands, 2116 Transvaal.
† Premier Mine, De Beers Consolidated Mines, P.O. Box 44, Cullinan, 1000 Transvaal.

 SA ISSN 0038-223X/3.00 + 0.00. Paper received October 1991; revised paper received June 1992.

INTRODUCTION

The tunnel support systems on Premier Mine are required, in terms of the current standard, to be designed beforehand and installed as an integral part of the mining process. Owing to the consequent support quantities and costs, and the impact on budgets and operational logistics, the underlying design needed to be reliable and comprehensive. No design system, either empirical or rigorous, was available for this purpose.

Rose[1] confirmed this situation in a survey of the design procedures adopted in applications of shotcrete reinforced with steel fibre and in the new Austrian tunnelling method, NATM. He found that no one used rigorous design methods and that the thickness of shotcrete was chosen empirically and was visually checked on construction for adequacy. In terms of the NATM, rockbolts and anchors are augmented continuously until displacements of the rockmass are arrested. Such approaches were neither practically feasible nor acceptable to the Mine.

The current mine-support standard is based on the Q-NATM system[2]. It is an empirical system of rockmass classification that does not enable the variation in support load around the tunnel and the depth of the support to be determined. The Q-NATM system allows consideration of the degree to which the rock may be over-stressed as a measure of displacement determinateness in terms of the stress-reduction factor, *SRF*. However, it does not permit determination of the degree of such over-stress as a function of depth. The size of the excavation is also not accounted for with sufficient sensitivity, and the shape of the excavation not at all.

The objective was accordingly to develop a rigorous design system with which the adequacy of the current standard could be checked in regard to these shortcomings and on which future support designs could be based.

The two-dimensional FLAC numerical simulation scheme[3] was used for this purpose. Owing to the complexity of the problem, the study was confined to a two-dimensional evaluation of the main production tunnels.

The symbols and abbreviations adopted in this paper are defined in Addendum 1. The term *shotcrete* is used interchangeably to denote either shotcrete or concrete in any of the walls of a tunnel.

MINE GEOLOGY

According to Knight[4], the seven main types of rock in the BA5 block comprise tuffisitic brown and grey kimberlite breccia, hypabyssal brown and black kimberlite, pale and dark piebald kimberlite, and carbonate dykes associated with the hypabyssal black kimberlite. The grey kimberlite breccia is extensively decomposed around the pipe contact and, as an intrinsically squeezing rock, was the subject of the study. The various rock types can be arranged into four main categories for the purposes of defining typical rockmass parameters. These are tuffisitic brown and decomposed grey kimberlite breccia; tuffisitic grey kimberlite breccia; hypabyssal brown, pale, and dark piebald kimberlite; and hypabyssal black kimberlite and associated carbonate dykes. The geological characteristics and rockmass parameters used for the determination of Q and *SRF* for the tuffisitic kimberlite breccia can be summarized as follows.

Three sets of joints of random orientation occur in the breccia. The joints are spaced on average at 150 mm, are rough and wavy, 90 per cent closed, and 10 per cent filled with 1 to 2 mm of calcite gouge. The joints are mostly 1 to 3 m long. The *RQD* varies from 35 to 72 per cent, and the unconfined compressive strength from 65 to 98 MPa.

MINING LAYOUT

The main levels in the BA5 block cave comprise the undercut level at elevation 615 m, the production level at elevation 630 m, and the haulage and ventilation level at elevation 645 m. A typical layout of the tunnels on the production level is shown in Figure 1.

The primary excavation units on the production level comprise the main and cross-cut tunnels; the acute and oblique corners formed at the intersections between those tunnels, referred to as bullnoses and camelbacks respectively; and the draw-point portals to the crosscut tunnels at the bases of the troughs. The bodies of rock traversed by the main tunnels are referred to as the main pillars.

TUNNEL SIZES AND LAYOUT GEOMETRY

Seven D-shaped sizes of tunnel were considered of height x width 2,8 x 2,8 m; 3,01 x 3,5 m; 4,0 x 4,2 m; 4,0 x 5,2 m; 4,0 x 6,5 m; 5,0 x 6,5m; and 6,0 x 6,5 m respectively. The first four of these sizes were 30 m apart between centres, and the last three 34 m.

According to Esterhuizen[5], the staggered offsets and angled directions of the crosscuts on alternate sides of the main tunnels shown in Figure 1 ensure a reasonably uniform state of mining-induced field stress in the main pillars. The tunnels were accordingly assumed to be

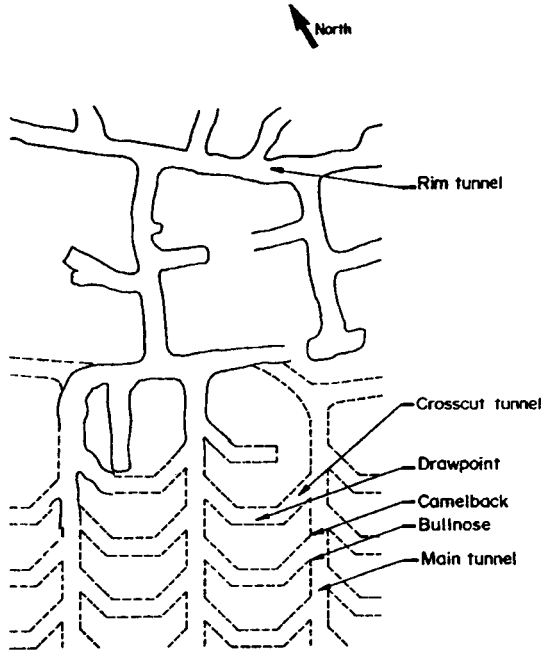

Figure 1—Typical layout of tunnels on the production level in BA5 block cave

amenable to two-dimensional analysis, and the main pillars to be of infinite extent in terms of the field in which the tunnels are excavated.

MINING SEQUENCE AND FIELD STRESSES

The tunnels on the production level are the first excavations installed in the block. Then the troughs are installed, the undercut retreated, and the ore drawn until the cave is exhausted. The corresponding loading stages are referred to as initial development, excavation of troughs, retreat of undercut, and cave exhausted.

The heads of rock at the production level, representing the various stages, were assumed, on the basis of analyses carried out by Esterhuizen[5], to amount to 265 m, 630 m, 1325 m, and 63 m. The production level is 630 m below natural ground level. It was shown by Kirsten *et al.*[6], in a qualitative evaluation of the failure patterns in the tunnels on adjoining levels, that the horizontal field stress in the pipe on this level corresponds to the natural depth below surface. The head of rock in respect of the horizontal field stress was accordingly taken as 630 m for all the stress stages.

The *SRF* values were accordingly determined as 6,64; 4,52; 16,98; and 10,51, which, according to Kirsten[7], represented mildly to minimally squeezing conditions for the first two loading stages and heavily squeezing conditions for the last two loading stages. The values for Q amounted to 0,87; 1,18; 0,34; and 0,53 for the four loading stages respectively.

FLAC SOLUTION SCHEME

The FLAC program was used for the numerical simulation of the various support configurations, and for the determination of the cohesion for the tuffisitic kimberlite breccia by quantitative back analysis of field-displacement data as described in Addendum 2.

The program is formulated in terms of an explicit finite-difference process, and allows two-dimensional stresses and displacements to be simulated. Initial coordinates of particles are taken as independent variables, which allows deformations of considerable magnitude to be modelled. The explicit nature of the process enables the propagation of disturbances to be simulated in increments just as it occurs in reality. This obviates the use of large matrices of simultaneous equations and the associated computing capacity, but is achieved at the expense of considerable run times for solutions.

The explicit nature of the process also renders the simulation of non-linear constitutive laws comparatively easy, and ensures that local material failure and the inclusion of oddly shaped non-homogeneous bodies, such as elongated reinforcing elements, do not give rise to numerical instabilities.

Three constitutive models are provided in the program, in which the plastic state is preceded by linear elastic behaviour. The first model, which was used for the purposes of this study, is based on a Mohr–Coulomb yield function, and allows perfect plastic straining in terms of constant values for the friction and dilation angles.

Version 2.01 of the programme was used on a 640 k RAM x 286 machine, which in terms of memory capacity allowed a maximum of 1750 zones to be specified, a zone being the area demarcated by adjoining nodes.

MODELLING GRID AND BOUNDARY CONDITIONS

The domains of zones and boundary conditions for the model are shown in Figure 2. The vertical boundaries were 15 m and 17 m apart, depending upon the distance between the tunnels, and the top and bottom boundaries were approximately ten times the equivalent tunnel diameter above and below their centres. The model was divided into eighteen domains of uniformly sized zones. This allowed the finely divided zones close to the tunnel boundaries to be appropriately increased in size towards the remote boundaries. The domains immediately surrounding the tunnel were large enough to accommodate the 6,0 m long cable anchors.

Simulation of the initial development stage involved three computational phases. For the first of these, the tunnel excavation was omitted, vertical and horizontal stresses were initialized at every grid node, and the remote boundaries were fixed against normal displacement and freed in respect of tangential displacement. The initialized stresses included for gravity increased linearly over the height of the model relative to natural ground level, so that equivalent heads of rock of 265 m and 630 m obtained at the elevation of the footwall of the tunnel. The displacements resulting at the end of this phase were set equal to zero, being primitive in nature. The tunnel

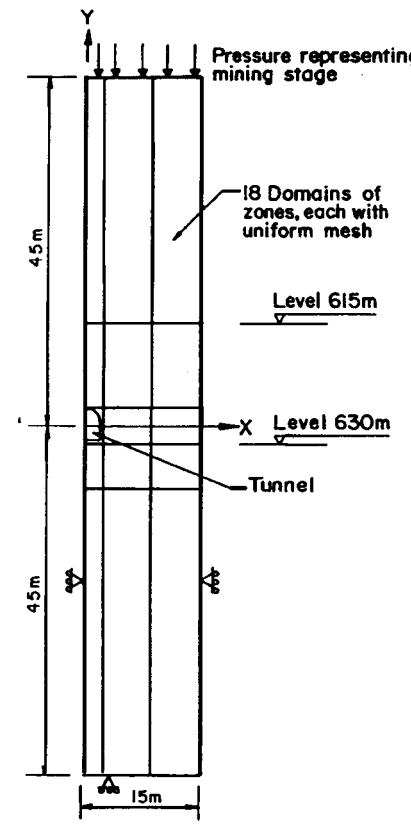

Figure 2—Configuration of numerical model with regard to domains and boundary conditions

excavation and entirely elastic material properties were introduced for the second phase. The full complement of support was introduced in the third phase, and the stresses were allowed to relax to within the specified Mohr–Coulomb envelope.

The rockbolts and cable anchors were introduced as fully grouted elastic—ideally plastic elements, the relevant elastic moduli, ultimate strengths, cross-sectional areas, and bond stiffnesses being fully operative throughout the various field-stress stages. The shotcrete was introduced as infinitely elastic fixed-end beam elements, and its elastic modulus, thickness, and second moment of area were specified.

The subsequent field-stress stages (excavation of troughs, retreat of undercut, and exhaustion of cave) were simulated by the application of equivalent uniformly distributed normal loads to the top boundary of the model so that the total vertical stresses at the elevation of the footwall of the tunnels corresponded to the respective heads of rock referred to. The material higher than elevation 615 m was assumed to represent caved ore from the retreat-of-undercut stage onwards, and was assigned a 10 per cent lower modulus at the start of this stage.

SUPPORT CONFIGURATIONS ANALYSED

The support configurations analysed for the various tunnel sizes are detailed in Table I. These comprise two

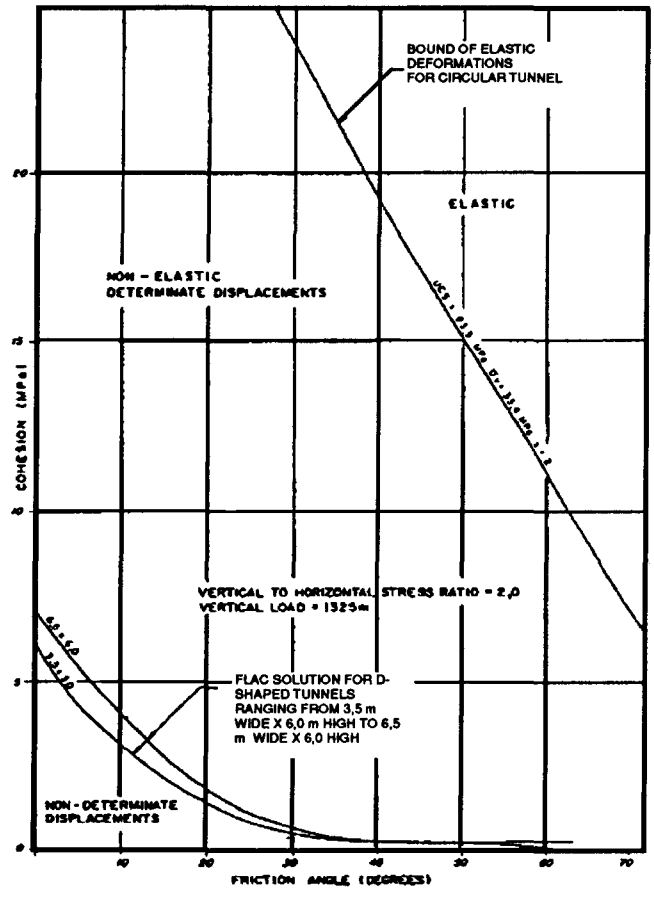

Figure 3—Relationships between cohesion and friction angle demarcating categories of displacement

categories: empirical support based on the Q-NATM system, and basic support. The empirical support comprised 1,8 m long fully grouted rockbolts in all walls on a 1,0 m square grid, 6,0 m long fully grouted cable anchors of 25 T capacity on a 2,0 m square grid, and 150 mm of mesh-reinforced shotcrete in the hanging- and sidewalls. The basic support consisted only of 1,8 m long fully grouted rockbolts and 6,0 m long fully grouted anchors both on 1,0 m square grids, in all walls and of unlimited tensile and bond strengths.

Two values, 200 GPa and 45 GPa, were considered for Young's modulus of the anchors in the basic support system. These respectively represented the steel strand normally used for anchors and glass fibre. The latter is a novel patented product that became available recently.

Various thicknesses of shotcrete, invert concrete arches, and intensities for the anchors in the footwall were considered in the case of the empirical support. In some instances, the footwall support was omitted, the footwall shotcrete stress-relieved, or the rock reinforcement optimized.

MANIFESTATION OF SQUEEZING CONDITIONS IN NUMERICAL MODELS

The displacements in a rockmass continuum fall into three categories: elastic, determinate plastic, and indeterminate plastic. Elastic and determinate plastic displacements are related directly to the loading that gives rise to them, and occur simultaneously with the load. Indeterminate plastic displacements do not cease after the load is fully applied, but continue to increase as long as the load is maintained. The squeezing displacements that are observed in actual excavations are of an on-going, indeterminate plastic nature.

Displacement indeterminacy occurs in numerical models when the stress–strain properties of the material are such that the physical laws on which the models are based cannot be satisfied. In QUAD[8], this is manifest as an inability of the solution to converge and, in FLAC[3], as a non-slowing of nodal perturbations. The values for the material properties at the onset of such conditions in the numerical solution schemes represent lower bounds.

A direct relationship exists between the compatibility between the stress–strain properties and the physical laws in numerical models, and the stress–strain properties and the physical laws in actual situations. The lower bounds that can be determined for stress–strain parameters from displacement indeterminacies in models are therefore representative lower bounds for the stress–strain parameters for the actual material.

Two sizes of D-shaped tunnel (3,0 x 3,5 m and 6,0 x 6,5 m) were simulated with FLAC to determine such lower bounds for the tuffisitic kimberlite breccia. A vertical-to- horizontal field-stress ratio of 1325 to 630 = 2,1 was considered in the analyses. The material was assumed to be joint free, and to have a Young's modulus of 5 GPa and a Poisson's ratio of 0,2. The onset of indeterminate displacements was determined in terms of the acceleration of nodal perturbation from a series of analyses for different values of cohesion and friction angle, as shown in Figure 3.

Two relationships between cohesion and friction angle

Table 1

Support configurations analysed for various sizes of tunnel

Item	Support configuration	Tunnel height x width m x m						
		2,8 x 2,8	3,0 x 3,5	4,0 x 4,2	4,0 x 5,2	4,0 x 6,5	5,0 x 6,5	6,0 x 6,5
1	Emp supp with 30 fw sc	√	√	√1				√1
2	Emp supp with fw anchors doubled		√2	√2				
3	Emp supp with fw supp omitted		√					√
4	Emp supp with 150 fw sc, but fw reinf omitted			√				
5	Emp supp with 300 fw sc, but fw reinf omitted							√
6	Emp supp equiv circ tunnel with 150 sc all walls			√				
7	Emp supp with 150 sc inv arch			√				
8	Basic supp with 1,8 m anchors		√3					
9	Basic supp with 3,0 m anchors		√3		√3		√3	
10	Basic supp with 4,5 m anchors		√3		√3			
11	Basic supp with 6,0 m anchors	√4	√3,4	√3,4	√3,4	√3	√3	√3,4
12	Basic supp with 8,0 m anchors						√3	
13	Basic supp with 150 sc all walls		√	√5				√5
14	Basic supp with 150 sc all walls, multiple stress relieved		√					
15	Basic supp with 300 sc all walls, multiple stress relieved		√3	√3	√3	√3	√3	√3
16	Basic supp with 600 sc all walls, multiple stress relieved							√
17	Totally unsupported	√	√	√	√	√	√	√
18	Basic supp with 150 sc all walls, but fw reinf omitted		√					
19	Basic supp with 300 sc all walls, but fw reinf omitted			√				
20	Basic supp with 600 sc all walls, but fw reinf omitted							√
21	Basic supp with 150 sc part sw and fw slotted and fw reinf omitted		√					
22	Basic supp with 300 sc part sw and fw slotted and fw reinf omitted			√	√			
23	Basic supp with 600 sc part sw and fv slotted and fw reinf omitted							√
24	Basic supp with 300 sc all walls multiple stress relieved for c = 1,5 MPa			√				
25	Basic supp with 600 sc all walls multiple stress relieved for c = 1,5 MPa							

Notes:
1 Also for 150 and 300 fw sc.
2 Also for fw anchors quadrupled.
3 Also for glass-fibre anchors.
4 Also fw reinf omitted.
5 Also for 300, 600, and 1000 sc.

Key:
circ = circular
emp = empirical
equiv = equivalent
fw = footwall
inv = invert
reinf = reinforcement
sc = shotcrete
supp = support
sw = sidewall

are illustrated in Figure 3. The top one distinguishes elastic from determinate plastic displacements, and the bottom one determinate plastic from indeterminate plastic displacements. The bottom boundary was not very sensitive to excavation size.

ROCKMASS PROPERTIES SIMULATED

The stress–strain properties adopted for the tuffisitic kimberlite breccia in the numerical analyses are given under the heading 'Rockmass' in Table II. These were determined in three alternative ways. Arbitrary assessments, results of small-scale laboratory tests, and classification parameters were used in the first instance as presented in Addendum 2. Alternative estimates were made of the peak cohesion as presented in the same Addendum in terms of a quantitative back-analysis of field displacements and a qualitative evaluation of the onset of indeterminate displacements respectively.

Table II
Material properties of tuffisitic kimberlite breccia

Parameters	Intact rock	Rockmass
Density, T/m³	2,65	2,65
RQD, %	100	35 - 72
Q (3rd stage)	–	0,34 - 1,22
Young's modulus, GPa	20,0 - 30,7	2,1 - 8,3(1)
Poisson's ratio	0,2 - 0,28	0,2
Uniaxial compressive strength, MPa	66 - 95	–
Friction angle, °	55	30
Cohesion, MPa	10,4 - 15,0	1,1 – 4,0(2)

Notes:
(1) Taken 5,0 GPa
(2) Taken 0,5 MPa

RIGOROUS SHOTCRETE AND MESH DESIGN

The FLAC solution scheme enables the moments and thrusts to which the shotcrete is subjected to be determined. The capacity of the shotcrete, in terms of thickness and reinforcement content to withstand such forces, can be determined from appropriate analyses of ultimate strength as presented by Kirsten[9].

It may not be possible under conditions of extreme deformation to economically design the reinforced shotcrete as an intact element. On the assumption that the shotcrete has completely failed or that it is not relied upon under such circumstances, mesh can be considered to support the rock surface as a uniformly loaded parabolic catenary spanning between the bolt and anchor heads, also as presented by Kirsten[9].

SUPPORT CHARACTERISTICS IDENTIFIED

The various tunnel configurations numerically simulated enabled the following support characteristics to be identified.

Interaction between Shotcrete and Rock

Shotcrete constitutes a confined inclusion and, in an intact condition, is considerably stiffer than rock reinforcement. It consequently attracts such a large proportion of the load that it may be subject to failure at various locations around the tunnel, depending on the magnitude of the field-stress state relative to the strength and deformability of the surrounding rockmass. These observations are illustrated in Figures 4 and 5, in which the distributions in reinforcement load with and without shotcrete for the 4,0 x 4,2 m tunnel subject to the retreat-of-undercut stage are shown respectively. The reinforcement loads are evidently very much reduced by the inclusion of the shotcrete. The direct compressive stresses in the shotcrete are generally of the order of 100 MPa, which is far greater than the strength usually obtained for shotcrete in underground applications.

Curvature of Shotcrete

Curvature increases the stiffness of the shotcrete and therefore its avidity for load. Distributions of in-plane shotcrete thrusts for a 4,0 x 4,2 m D-shaped tunnel, a 4,0 x 4,2 m D-shaped tunnel provided with an arched invert, and a tunnel of equivalent circular dimension, all provided with 150 mm of shotcrete and the mine standard support, and subject to the retreat-of-undercut stage, are shown in Figure 6. It is evident that the shotcrete linings of greater curvature are subject to greater stresses.

Stiffness of Shotcrete as a Function of Thickness

The thrusts and direct stresses in the crowns of shotcrete linings of various thickness, applied in addition to the basic support in various sizes of tunnel, are presented in Table III. The shotcrete stresses for a 4,0 x 4,2 m tunnel are plotted against thickness in Figure 7.

It is evident from Table III that the relative stiffness of intact shotcrete increases with an increase in thickness for all tunnel sizes, but at a lesser rate than the increase in thickness itself. Therefore, although increments in thickness attract larger loads, the corresponding stresses are reduced with an increase in thickness.

The extent to which the relative stiffness of shotcrete increases with an increase in thickness becomes insignificant beyond a characteristic thickness for any given field situation (Figure 7). A characteristic minimum stress that is asymptotically approached by an increase in thickness may, as a result, be identified for any given field situation. A characteristic thickness may, in turn, be identified in terms of a particular level of stress for a

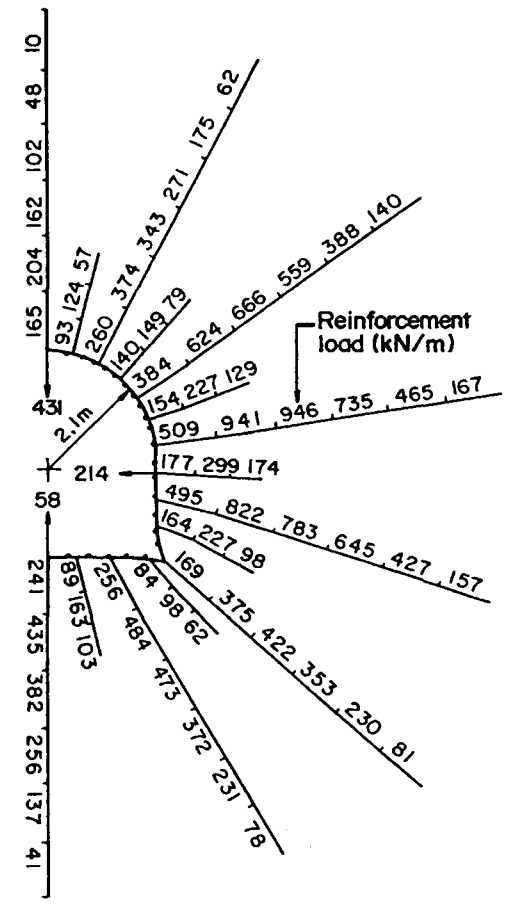

Figure 4—Distribution of reinforcement load for a 4,0 x 4,2 m basically supported tunnel subject to the retreat-of-undercut stage

Table III

Thrusts and direct stresses in crown of shotcrete in basically supported tunnels of various sizes

Mining stage	Thickness	Thrust, MN/m Tunnel height x width m x m			Direct stress, MPa Tunnel height x width m x m		
	mm	3,0 x 3,5	4,0 x 4,2	6,0 x 6,5	3,0 x 3,5	4,0 x 4,2	6,0 x 6,5
Initial development	150	8,24	9,22	11,43	55	62	76
	300	–	9,82	13,72	–	33	46
	600	–	9,53	14,75	–	16	25
	1 000	–	9,54	14,64	–	10	15
Excavation of troughs	150	10,53	11,20	12,53	70	75	84
	300	–	14,46	18,01	–	48	60
	600	–	17,00	22,88	–	28	38
	1000	–	18,84	25,75	–	19	26
Retreat of undercut	150	13,81	13,24	16,32	92	88	109
	300	–	22,73	24,03	–	76	80
	600	–	30,62	39,06	–	51	65
	1000	–	36,76	48,63	–	37	49
Point loading	150	–	–	–	–	–	–
	300	–	–	–	–	–	–
	600	–	–	–	–	–	–
	1 000	–	–	–	–	–	–
Cave exhausted	150	1,28	6,01	9,18	9	40	61
	300	–	4,66	14,33	–	16	48
	600	–	10,63	15,13	–	18	25
	1 000	–	7,42	1,08	–	7	1

particular field situation. Increases in field stress give rise to considerably increased characteristic minimum stresses and, as a result, to considerably increased characteristic thicknesses for particular levels of stress.

CHARACTERISTIC MINIMUM SHOTCRETE STRESS AND THICKNESS

The characteristic minimum stresses and thicknesses for shotcrete as intact medium are given in Table IV for two of the tunnel sizes and the four mining stages considered. These were determined from numerical simulations of the tunnels provided with the basic support and different thicknesses of shotcrete. In those instances in which the minimum stress is less than 25 MPa (an arbitrary limit), the thickness corresponding to 25 MPa is given in brackets. It is evident that the minimum shotcrete stresses are generally acceptable, but the corresponding thicknesses are not. Even in those instances in which the minimum stress is raised to 25 MPa, the corresponding reduced thicknesses are generally still far too large for practical purposes. It is also evident that the shotcrete stresses and thicknesses are sensitive to the magnitudes of the field stresses.

Modulus of Shotcrete

A change in the modulus of the shotcrete is directly equivalent to a change in thickness. The earlier comments with regard to thickness therefore apply equally well to modulus as confirmed in Figure 8, which shows the stress distributions for different Young's moduli for the shotcrete in a circular tunnel of diameter equivalent to the 4,0 x 4,2 m tunnel, provided with the mine standard support and subject to the retreat-of-undercut stage.

Relative Support Roles of Shotcrete and Rock Reinforcement

If either the characteristic minimum stress or the thickness is not acceptable under squeezing conditions, the shotcrete should be appropriately relieved in the design process of undue thrusts. Under such circumstances, the shotcrete serves as secondary support of the rock surface between adjoining anchors, and is subject mainly to bending. On the failure of the shotcrete in bending, the mesh is subject to catenary action. The deeply penetrating rock reinforcement at the same time constitutes the primary support, responsible for the global stability and overall displacement control of the excavation.

Field-stress Effects

A change in field stress from one mining stage to another displaces the ground surrounding the tunnels to various degrees, depending upon the distance from the tunnel, the position around the tunnel, the shape of the tunnel, and the type of support.

An increment in the vertical stress on the undercut level generally displaces the tunnel bodily downwards. As a result, the ends of the reinforcement in the upper part of a

Table IV

Minimum stresses and thicknesses of shotcrete in crown for various tunnel sizes and mining stages

Mining stage	Minimum shotcrete stresses, MPa Tunnel height x width m x m		Minimum shotcrete thicknesses, mm Tunnel height x width m x m	
	4,0 x 4,2	6,0 x 6,5	4,0 x 4,2	6,0 x 6,5
Initial development	7 (25)	11 (25)	1600 (420)	1800 (600)
Excavation of troughs	14 (25)	19 (25)	1600 (680)	1800 (1040)
Retreat of undercut	29	37	1600	1800
Cave exhausted	3 (25)	0	1600 (230)	1050 (630)

tunnel are displaced in similar directions, and in the lower part in different directions. The corresponding distributions in reinforcement load for a 4,0 x 4,2 m tunnel provided

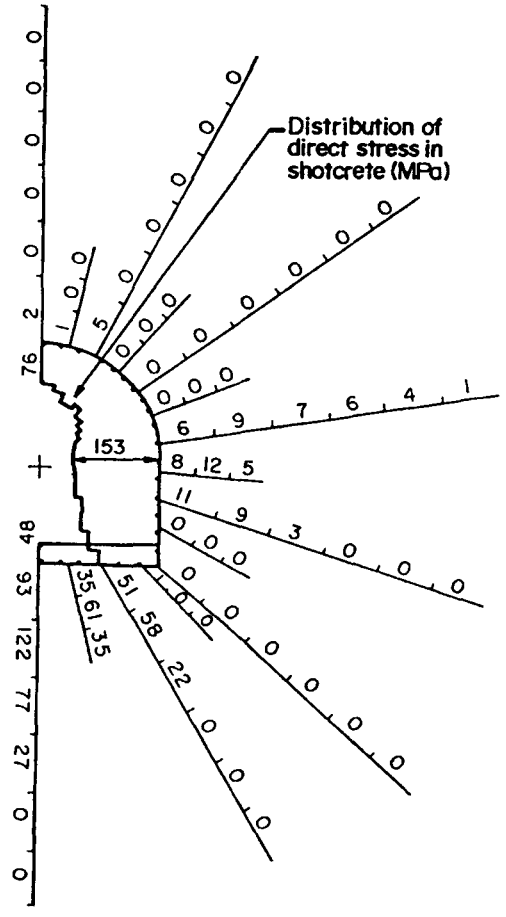

Figure 5—Distribution of reinforcement load for a 4,0 x 4,2 m basically supported tunnel with 300 mm of shotcrete, subject to the retreat-of-undercut stage

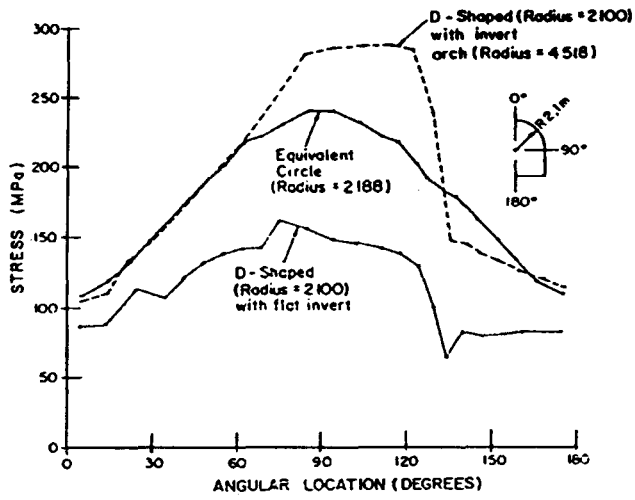

Figure 6—Distribution of shotcrete stress for variously shaped 4,0 x 4,2 m empirically supported tunnels with 150 mm of shotcrete, subject to the retreat-of-undercut stage

with the basic support and subject to the retreat-of-undercut stage are illustrated in Figure 4.

A reduction in the vertical stress on the undercut level, as occurs during the cave-exhausted stage, has the reverse effect of displacing the tunnel bodily upwards. As a result, the back ends of the reinforcement in the upper part of the tunnel are displaced upwards, and the reinforcement load increases correspondingly, as illustrated in Figure 9. The heads of the reinforcement in the footwall of the tunnel are displaced upwards to a greater extent than the back ends, which also gives rise to equally great increases in reinforcement load.

Field-Stress Governing Support Design

The loads in the reinforcement generally increase with an increase in the vertical field stress over the successive mining stages, as shown in Figure 10, in which the distributions of maximum reinforcement load for the

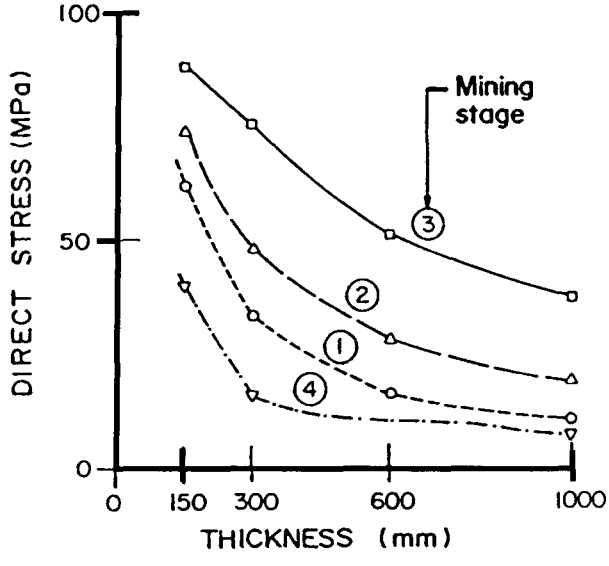

Figure 7—Graphs of shotcrete crown stress against thickness for a 4,0 x 4,2 m basically supported tunnel subject to various mining stages

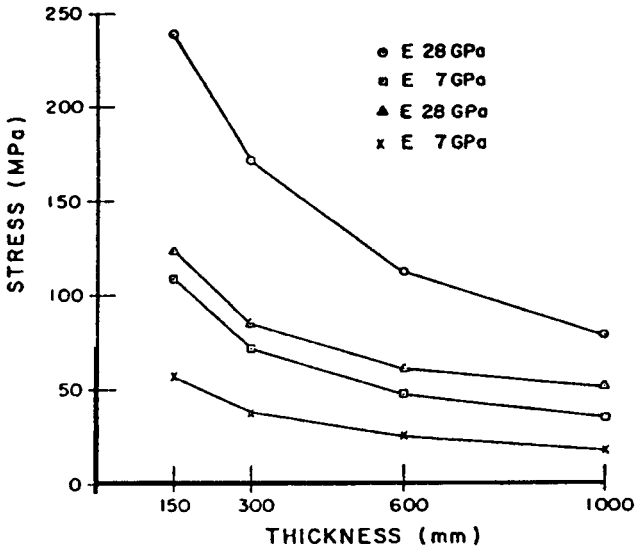

Figure 8—Graphs of shotcrete crown stress against thickness for various moduli for a circular empirically supported tunnel subject to the retreat-of-undercut stage

basically supported 4,0 x 4,2 m tunnel are given.

Distribution of Reinforcement Load

The reinforcement demands can be seen from Figure 10 to be the greatest in the sidewall for the main mining stages. These observations can be shown to hold irrespective of tunnel size.

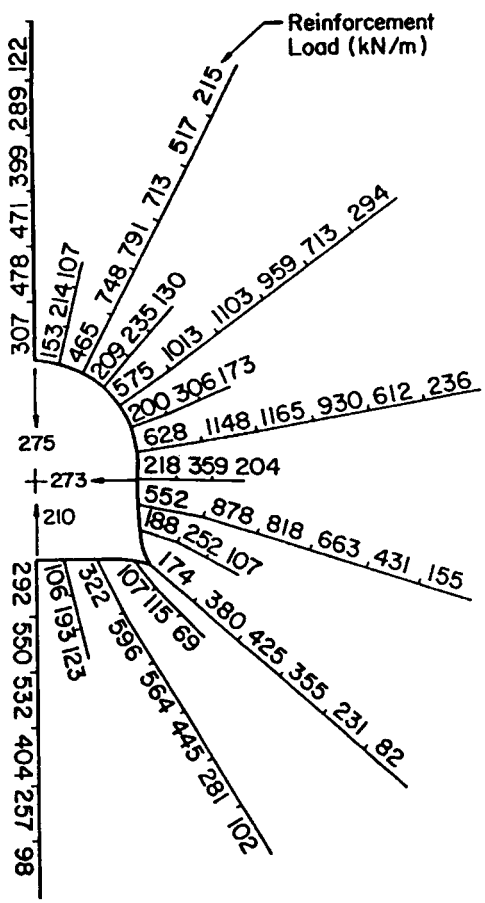

Figure 9—Distribution of reinforcement load for a 4,0 x 4,2 m basically supported tunnel subject to the cave-exhausted stage

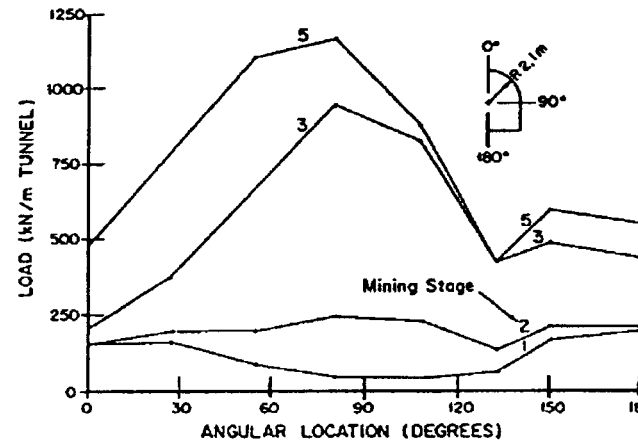

Figure 10—Distribution of maximum reinforcement load for a 4,0 x 4,2 m basically supported tunnel subject to various mining stages

Redistribution of Anchor Loads by Shotcrete

The distribution of maximum anchor loads for the various sizes of basically supported tunnel respectively without multiple stress-relieved shotcrete and with it are given in Tables V and VI for both the retreat-of-undercut and the cave-exhausted stages. It is evident that the mesh-reinforced shotcrete, despite being stress-relieved, substantially reduces the anchor loads in the sidewalls, and results in more uniform distributions in anchor load around the tunnels.

Tunnel Shape and Size

Figures 11 and 12 show the distributions of maximum reinforcement demand and the relative normal displacement for the various sizes of basically supported tunnel subject to the retreat-of-undercut stage. The corresponding distributions of relative normal displacement for the tunnels not provided with any support are shown in Figure 13.

It is evident from Figure 11 that the increase in reinforcement load in the sidewall due to an increase in tunnel height is considerably greater than that in the hanging- and footwalls due to an increase in tunnel width.

It is also evident from Figure 11, as well as from Table

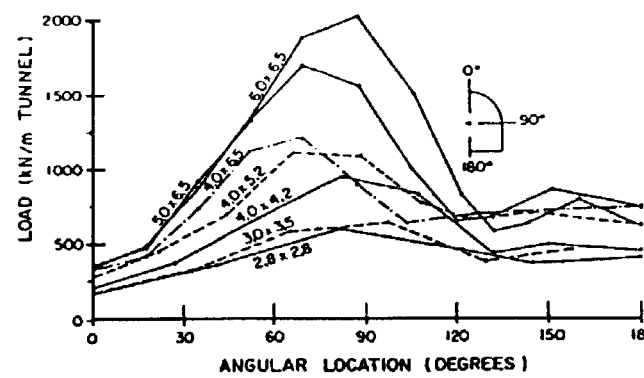

Figure 11—Distribution of maximum reinforcement load for various dimensions of basically supported tunnel subject to the retreat-of-undercut stage

Table V

Rigorously determined maximum steel anchor forces for various tunnel sizes provided with basic support in all walls

Tunnel height x width m x m	Maximum[1] force at position[2], T/m											
	1	2	3	4	5	6	7	8	9	10	11	12
2.8 x 2,8	17,4 (42,3)	35,8 (79,1)	59,6 (73,5)	45,4 (45,3)	35,5 (41,4)	39,2 (54,1)	–	–	–	–	–	–
3,0 x 3,5	16,5 (41,2)	31,9 (74,8)	57,3 (81,0)	63,3 (68,5)	37,6 (38,5)	44,7 (61,9)	–	–	–	–	–	–
4,0 x 4,2	20,4 (47,8)	37,4 (79, 1)	66,6 (110,3)	94,6 (114,8)	82,2 (87,8)	42,2 (42,5)	48,4 (59,6)	43,5 (55,0)	–	–	–	–
4,0 x 5,2	28,3 (71,1)	45,0 (98,5)	69,6 (129,1)	110,7 (147,2)	109,3 (123,1)	76,1 (76,3)	64,9 (65,2)	69,8 (78,1)	55,5 (74,3)	–	–	–
4,0 x 6,5	32,8 (67,0)	41,5 (80,2)	73,0 (126,2)	112,4 (156,0)	121,4 (144,1)	89,1 (97,7)	63,8 (64,6)	64,1 (63,7)	69,2 (77,6)	72,8 (82,7)	–	–
5,0 x 6,5	36,6 (70,3)	46,1 (86,8)	90,8 (153,7)	132,5 (182,5)	169,8 (196,5)	155,9 (170,3)	99,3 (103,0)	64,2 (64,1)	67,2 (70,7)	85,5 (94,7)	73,2 (80,3)	–
6,0 x 6,5	34,1 (64,6)	49,7 (92,4)	87,8 (150,4)	134,6 (182,1)	187,0 (213,2)	201,8 (215,6)	150,9 (157,2)	81,7 (82,7)	57,6 (59,1)	61,9 (65,8)	98,6 (87,2)	60,6 (67,4)

Notes:

(1) First entry refers to the retreat-of-undercut stage, and the second, in brackets, to the cave-exhausted stage

(2) Anchor/rockbolts located on a 1,0 m square grid. Circumferential positions numbered from centre of hangingwall down. The three domains shown designate, in order, the hanging-, side-, and footwalls

Table VI

Rigorously determined maximum steel anchor forces for various tunnel sizes provided with basic support in all walls and 300 mm of mesh-reinforced multiple stress-relieved shotcrete

Tunnel height x width m x m	Maximum[1] force at position[2], T/m											
	1	2	3	4	5	6	7	8	9	10	11	12
3,0 x 3,5	12,5 (44,3)	8,9 (72,3)	21,3 (44,8)	32,3 (31,7)	20,4 (18,9)	44,5 (61,6)	–	–	–	–	–	–
4,0 x 4,2	15,4 (48,0)	11,6 (78,8)	26,2 (81,7)	33,5 (54,4)	53,5 (63,2)	24,7 (24,5)	39,5 (49,7)	41,2 (56,5)	–	–	–	–
4,0 x 5,2	23,8 (63,5)	28,1 (114,8)	47,9 (129,8)	73,2 (131,1)	78,1 (100,7)	68,9 (84,7)	48,9 (46,1)	67,3 (76,1)	62,2 (79,4)	–	–	–
4,0 x 6,5	22,1 (56,6)	23,6 (82,5)	36,0 (103,0)	66,0 (115,9)	77,4 (117,5)	56,2 (64,4)	45,6 (42,0)	55,2 (51,3)	90,3 (97,2)	62,2 (70,9)	–	–
5,0 x 6,5	27,1 (57,7)	28,6 (98,5)	47,9 (130,7)	83,1 (157,7)	105,5 (156,5)	100,4 (125,0)	76,2 (98,9)	41,6 (39,0)	61,8 (60,9)	85,9 (96,6)	69,5 (78,1)	–
6,0 x 6,5	28,7 (40,7)	29,4 (53,0)	53,3 (77,5)	93,7 (112,2)	138,6 (152,6)	149,4 (156,6)	125,2 (125,0)	99,8 (97,2)	39,7 (34,9)	55,2 (50,1)	83,6 (81,3)	66,1 (65,2)

Notes:

(1) First entry refers to the retreat-of-undercut stage, and the second, in brackets, to the cave-exhausted stage

(2) Anchor/rockbolts located on a 1,0 m square grid. Circumferential positions numbered from centre of hangingwall down. The three domains shown designate, in order, the hanging-, side-, and footwalls

VI, that the anchor loads are prohibitively large for the larger sizes of tunnel. The actual size of tunnel for which the anchor loads become prohibitively large depends on the strength of the rockmass.

The relative normal convergences for tunnels basically supported are slightly more sensitive to changes in width than to changes in height. In neither instance, however, are the relative normal convergences significantly affected by changes in dimensions, as shown in Figure 12.

As evident in Figure 13, the relative normal displace-

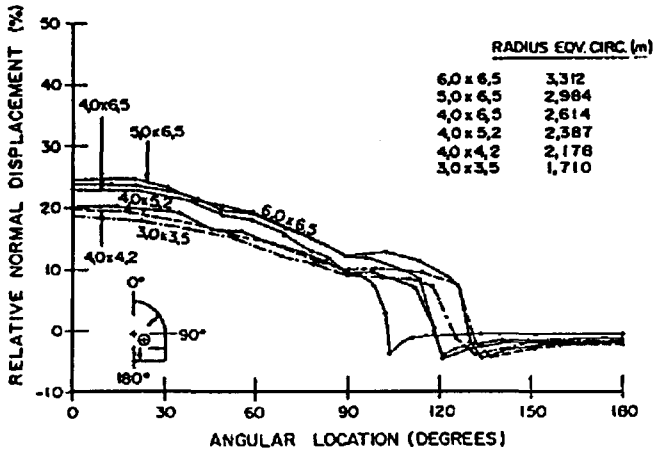

Figure 12—Distribution of relative normal displacement for various dimensions of basically supported tunnel subject to the retreat-of-undercut stage

ments in tunnels not provided with any support are very sensitive to tunnel dimensions, more so with regard to height than to width, and far more so for larger than for smaller tunnels. The relative normal displacements in the hanging-, side-, and footwall of the 3,0 x 3,5 m tunnel are, for example, reduced by the support from 22, 13, and 1 per cent to 18, 9, and –2 per cent respectively. The corresponding figures for the 6,0 x 6,5 m tunnel are 50, 40, and 15 per cent without support, and 24, 12, and –2 per cent with support respectively.

Distributions of the relative extents of the zones of failure around various sizes of unsupported tunnel subject to the retreat-of-undercut stage are shown in Figure 14. It is evident that the relative extent of the surrounding failed zones is generally equally sensitive to tunnel height and width.

Footwall Reinforcement

Figures 15 and 16 show, for the retreat-of-undercut stage, the distributions of maximum reinforcement demand and relative normal displacement for the various sizes of tunnel provided with the basic support in all but the footwall. It is evident from a comparison of these figures respectively

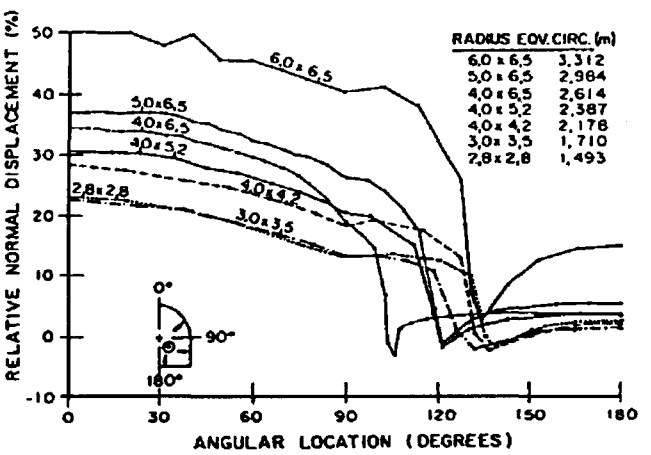

Figure 13—Distribution of relative normal displacement for various dimensions of unsupported tunnel subject to the retreat-of-undercut stage

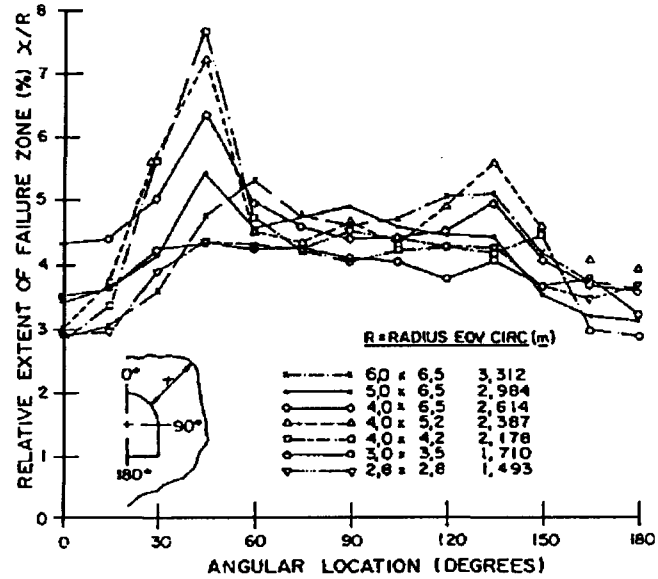

Figure 14—Distribution of relative extent of failure zone for various dimensions of unsupported tunnel subject to the retreat-of-undercut stage

with Figures 11 and 12 that omission of the footwall reinforcement does not significantly affect the reinforcement demands or convergences in any of the other walls. The relatively independent behaviour of the walls of the tunnels is due to the provision of reinforcement of unlimited tensile and bond strength. It is only when the reinforcement in any one wall is deficient that it becomes sensitive to the omission of reinforcement in any other wall.

The omission of reinforcement from any wall depends on the creep behaviour of the rock. If unsupported, a particular wall may be subject to on-going creep that, if continuously sliped or shaved, will eventually result in undermining of the reinforcement in adjoining walls.

Modulus of Anchors

Figures 17 and 18 show the distributions of maximum reinforcement demand and relative normal displacement for the various sizes of tunnel basically supported with glass-fibre anchors and subject to the retreat-of-undercut stage. It is evident from a comparison of Figures 11 and 17 that the loads in the glass-fibre anchors are on average about 70 per cent of the loads in the steel anchors. The loads in the rockbolts used with glass-fibre anchors are generally 10 per cent larger than those in the rockbolts used with steel anchors.

The relative normal displacements for tunnels anchored with glass fibre can be seen from a comparison of Figures 12 and 18 to be 5 to 10 per cent greater than for steel-anchored tunnels.

Optimum Anchor Depth

Steel Anchors

The primary purpose of cable anchors is to curtail the indeterminate displacement of the plastically deformed rock, which varies in extent around a tunnel as a function of the field stresses. These stresses, in turn, vary from one mining stage to the next, as a result of which the problem

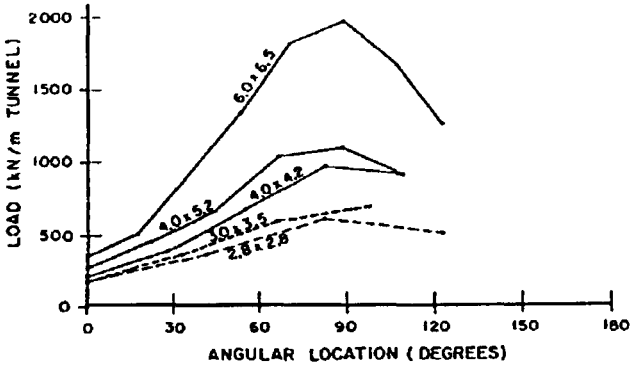

Figure 15—Distribution of maximum reinforcement load for various dimensions of basically supported tunnel except in the footwall, subject to the retreat-of-undercut stage

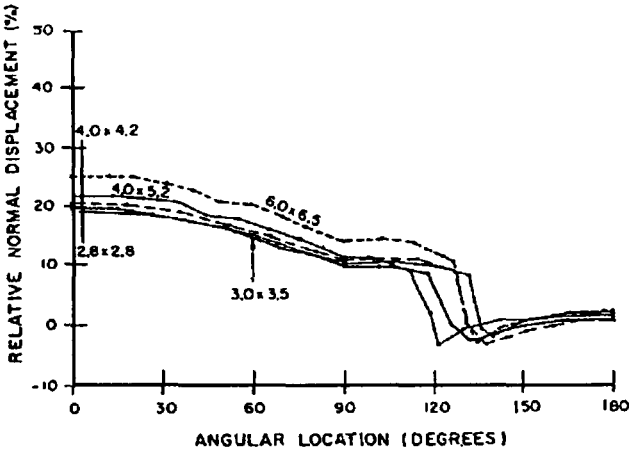

Figure 16—Distribution of relative normal displacement for various dimensions of basically supported tunnel except in the footwall, subject to the retreat-of-undercut stage

can be addressed only by the adoption of a uniform depth of anchor. To vary the depth of anchor around the tunnel would in any event not be practical. The object was, accordingly, to determine that uniform depth of anchor that would account for maximum conditions anywhere around the tunnel for any of the mining stages.

Three depths of anchor were considered for this purpose

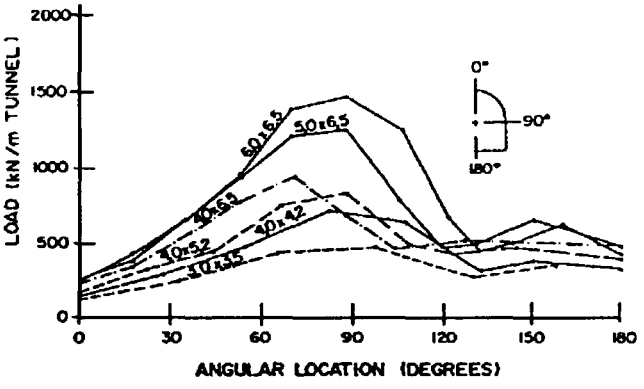

Figure 17—Distribution of maximum reinforcement load for various dimensions of tunnel basically supported with glass-fibre anchors and subject to the retreat-of-undercut stage

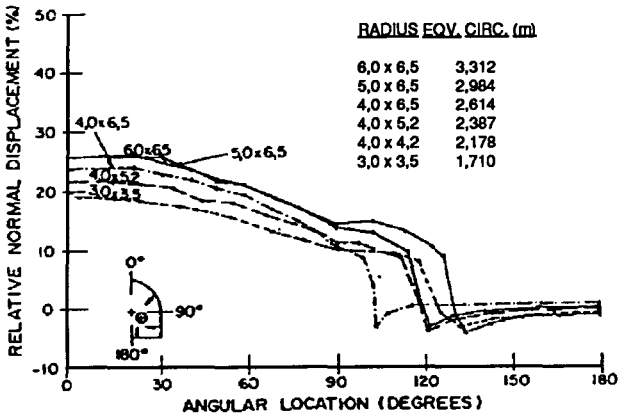

Figure 18—Distribution of relative normal displacement for various dimensions of tunnel basically supported with glass-fibre anchors and subject to the retreat-of-undercut stage

for each of three tunnel sizes: 1,8 m, 3,0 m, and 4,5 m long anchors for the 3,0 x 3,5 m tunnel; 3,0 m, 4,5 m, and 6,0 m long anchors for the 4,0 x 5,2 m tunnel; and 3,0 m, 6,0 m, and 8,0 m long anchors for the 5,0 x 6,5 m tunnel. The nominal relative depths of anchor amounted to 0,57; 0,97; and 1,35 for each of the three tunnel sizes.

The distributions of normal displacement, end anchor force, and maximum anchor force x length for the various depths of anchor and sizes of tunnel are given for the retreat-of-undercut stage in Figures 19, 20, and 21 respectively. The product of the force and length of an anchor is an inverse measure of efficiency.

It is evident from Figure 19 that the displacements are slightly reduced with increasing anchor depth, the rate of reduction becoming very small towards a relative depth of 1,35. As can be seen from Figure 20, the end anchor forces also decrease with increasing anchor depth, but not at a significantly changing rate. The shortest anchors are the

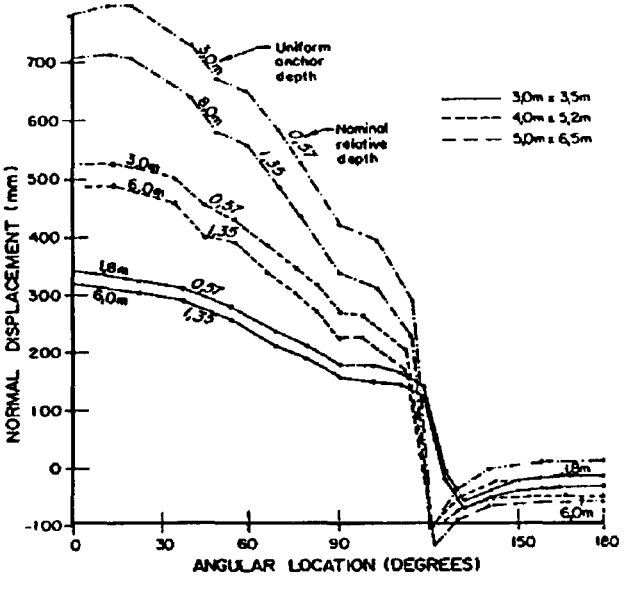

Figure 19—Distribution of normal displacement for various dimensions of tunnel basically supported with various lengths of steel end anchor, and subject to the retreat-of-undercut stage

most effective, as shown in Figure 21, because the forces increase with anchor depth.

Depending on the end anchor force, either the bond strength or the efficiency can be the criterion determining anchor depth. Bond strength is governed by the steel–grout interface being the weaker of the two interfaces that the grout respectively forms with the anchor and the surrounding rock. The steel–grout bond strength amounts to 440 kN/m for an equivalent solid-bar diameter of 25 mm. It is evident from Figure 20 that bond strength is the criterion for the larger sizes of tunnel but not for the smaller tunnels, for which efficiency is the criterion. For the larger tunnels, a relative depth of 1,37 will satisfy the bond strength, whereas the shortest anchor will suffice as the most efficient for the smaller tunnels, displacements permitting.

Glass-fibre Anchors

The distributions of normal displacement, end anchor force, and maximum anchor force x length for various depths of glass-fibre anchor and sizes of tunnel are given in Figures 22, 23, and 24 respectively for the retreat-of-undercut stage.

The same observations in principle apply to these diagrams as given earlier in respect of the steel anchors. The bond strength of the glass-fibre grout amounts to 280 kN/m for a solid-bar diameter of 22 mm. This is satisfied by a relative depth of anchor of 1,57 for the larger sizes of tunnel, which is larger than the relative anchor depth required for steel, 1,37.

Despite this observation, glass fibre is 25 per cent more effective than steel in terms of the product force x length, because the forces associated with glass fibre are so much smaller than those associated with steel. Indeed, the reduced forces associated with glass fibre permit the consideration of tunnel sizes that would not be practically feasible with steel.

Strength and Efficiency of Grouting of Reinforcement

The distributions of displacement and maximum anchor and bolt forces for a 4,0 x 4,2 m tunnel provided with basic

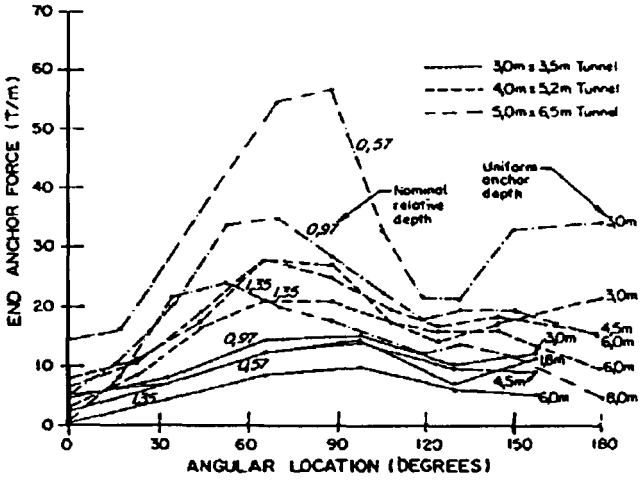

Figure 20—Distribution of end anchor force for various dimensions of tunnel basically supported with various lengths of steel anchor and subject to the retreat-of-undercut stage

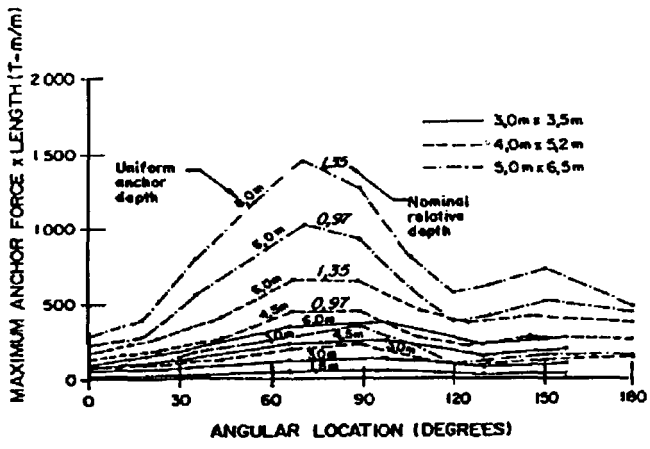

Figure 21—Distribution of maximum anchor force x anchor depth for various dimensions of tunnel basically supported with various lengths of steel anchor and subject to the retreat-of-undercut stage

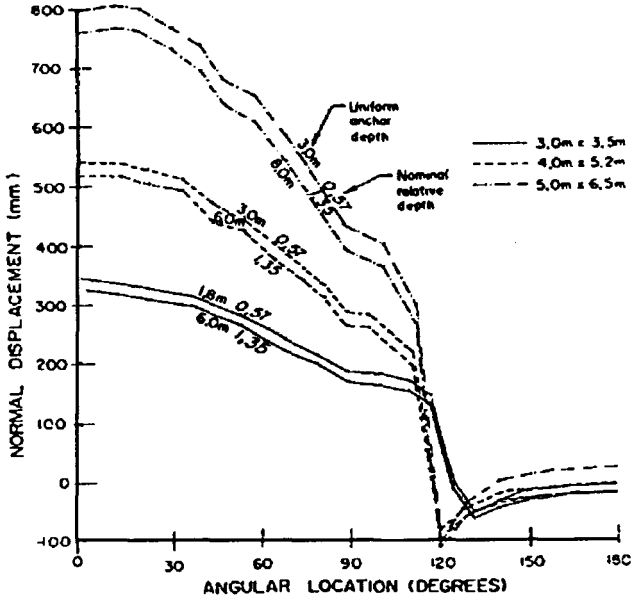

Figure 22—Distribution of normal displacement for various dimensions of tunnel basically supported with various lengths of glass-fibre anchor and subject to the retreat-of-undercut stage

support of varying bond strength are given in Tables VII and VIII for the retreat-of-undercut and cave-exhausted stages. It is evident from Table VII that the magnitude and distribution of anchor force are related to bond strength up to 1250 kN/m, at which value the distribution of anchor force is very uneven. A uniform distribution in anchor force of considerably reduced maximum value is obtained at a bond strength of 1000 kN/m. Although two of the anchors become debonded in the sidewall over the first 1,0 to 1,5 m at this value for bond strength, the displacements of the excavation wall are not affected. This is due to the effective overlap between the bolts and the anchors over the lengths over which the anchors are debonded. The intervening rock effectively splices the bolts to the anchors and, as such, comprises a controlled yielding mechanism. The required capacity for the anchors can evidently be kept relatively

Table VII

Rigorously determined maximum steel anchor forces for a 4,0 m x 4,2 m tunnel provided with basic support in all walls

Bond strength kN/m	No. of anchors failed	Displacements, mm			Maximum[1] force at position[2], T/m							
		Crown	Side	Floor	1	2	3	4	5	6	7	8
500	6	-475	-345	-18	25,7	29,2	22,2	105,5	32,5	54,3	23,0	19,0
	(7)	(-456)	(-436)	(139)	(22,5)	(63,1)	(27,9)	(30,3)	(22,3)	(52,1)	(23,3)	(16,9)
750	3	-416	-261	-50	23,0	43,5	37,8	38,3	34,8	48,5	51,8	46,7
	(4)	(-391)	(-369)	(169)	(38,5)	(50,6)	(74,1)	(22,4)	(30,3)	(46,3)	(61,5)	(56,8)
1000	2	-434	-219	-57	20,5	38,0	69,0	36,5	57,3	43,4	48,7	43,7
	(3)	(-287)	(-308)	(219)	(47,2)	(80,7)	(41,8)	(46,7)	(31,3)	(45,4)	(60,2)	(55,7)
1250	0	-432	-213	-59	20,3	37,5	67,4	94,0	82,0	42,2	48,6	43,5
	(1)	(-268)	(-272)	(217)	(48,2)	(80,2)	(112,7)	(43,8)	(87,9)	(42,7)	(58,8)	(54,9)
Un-limited	0	-431	-214	-58	20,4	37,4	66,6	94,6	82,2	42,2	48,4	43,5
	(0)	(-275)	(-273)	(210)	(47,8)	(79,1)	(110,3)	(116,5)	(87,8)	(42,5)	(59,6)	(55,0)

Notes:

(1) The first entry refers to the retreat-of-undercut stage and the second, in brackets, to the cave-exhausted stage

(2) Anchor/rockbolts located on 1,0 m square grid. Circumferential positions numbered from centre of hangingwall down

Table VIII

Rigorously determined maximum steel rockbolt forces for a 4,0 m x 4,2 m tunnel provided with basic support in all walls

Bond strength kN/m	No. of bolts failed	Maximum[1] force at positions[2], T/m						
		1	2	3	4	5	6	7
500	3	16,3	25,3	7,6	-	3,2	11,2	20,2
	(4)	(12,7)	-	(9,6)	-	(3,6)	(12,8)	(14,9)
750	0	14,4	18,3	26,3	36,3	27,1	10,0	17,7
	(3)	(17,1)	(25,2)	(11,1)	(17,9)	(19,1)	(11,7)	(20,4)
1000	0	12,6	15,7	23,0	31,0	22,8	9,8	16,5
	(0)	(19,1)	(23,9)	(34,0)	(42,6)	(28,4)	(11,9)	(19,7)
1250	0	12,5	15,5	22,3	30,0	22,4	9,8	16,4
	(0)	(22,0)	(23,8)	(30,0)	(35,7)	(25,0)	(11,4)	(19,3)
Un-limited	0	12,4	14,9	22,7	29,9	22,7	9,8	16,3
	(0)	(21,4)	(23,5)	(30,6)	(35,9)	(25,2)	(11,5)	(19,3)

Notes:

(1) The first entry refers to the retreat-of-undercut stage and the second, in brackets, to the cave-exhausted stage

(2) Anchor/rockbolts located on 1,0 m square grid. Circumferential positions numbered from centre of hangingwall down

small if the bond strength is limited to 1000 kN/m without invoking unduly adverse side effects.

Partial grouting represents an inefficiency that can be considered in terms of its effect on tunnel displacement and anchor force. If only the back halves of the anchors are grouted, the splicing effect between the bolts and anchors is absent, which results in a significant increase in the displacements and a large reduction in the anchor forces. If only the front halves of the anchors are grouted, the displacements are about 30 per cent larger and the maximum anchor forces about 50 per cent smaller because of the effective reduction in anchor length.

The effect of partial grouting is greatly dependent on the provision of separate end anchorages and face plates.

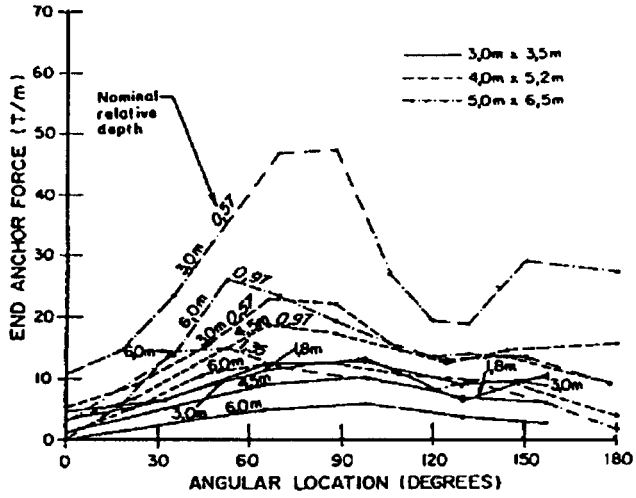

Figure 23—Distribution of end anchor force for various dimensions of tunnel basically supported with various lengths of glass-fibre anchor and subject to the retreat-of-undercut stage

Completely ungrouted anchors, end-anchored and provided with face plates, are subject to constant tensile forces about twice as large as the maximum forces in fully grouted anchors. The only effect of partially grouting either the front or back sections of anchors is to reduce the forces in the back sections to magnitudes comparable with those in the fully grouted case.

Rockmass Cohesion

The magnitude of the loads in the rock reinforcement depends on the strength of the surrounding rock. An increase in rockmass cohesion from 0,5 to 1,5 MPa results in an average reduction of 60 per cent in the reinforcement loads, as is evident from a comparison of Figures 4 and 25.

Appraisal of Empirically Determined Support

The distributions in reinforcement load, shotcrete stress, and convergence for the 4,0 x 4,2 m empirically supported tunnel subject to the retreat-of-undercut stage are given in Figure 26. It is evident that a significant proportion of the anchors and rockbolts in the side- and footwalls are broken.

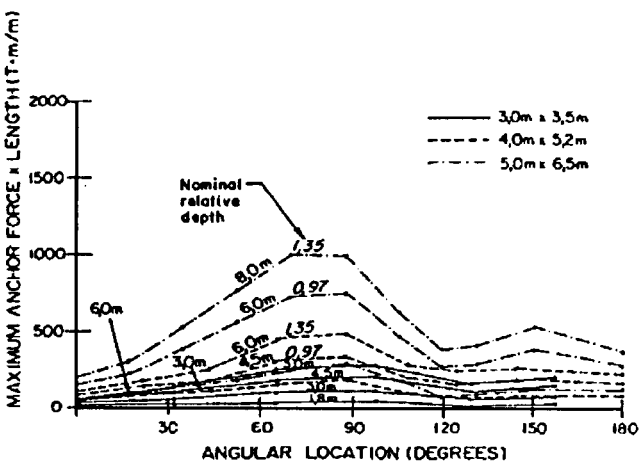

Figure 24—Distribution of maximum anchor force x anchor depth for various dimensions of tunnel basically supported with various lengths of glass-fibre anchor and subject to the retreat-of-undercut stage

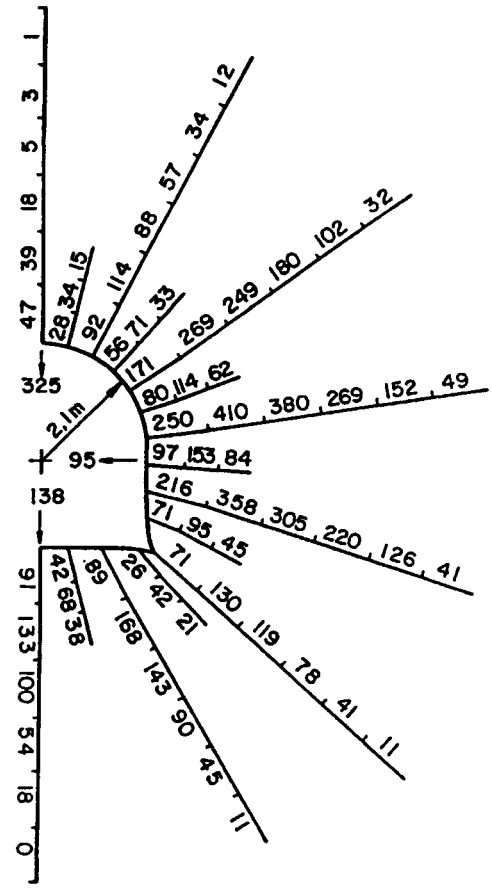

Figure 25—Distribution of reinforcement load for a 4,0 x 4,2 m basically supported tunnel subject to the retreat-of-undercut stage in a rockmass with a cohesion of 1,5 MPa

The shotcrete is also excessively stressed. The hanging- and sidewalls are substantially converged, and the footwall depressed. It can be shown that an even greater proportion of the rockbolts and anchors are broken, the shotcrete stressed to a lesser extent, the hangingwall convergence reduced, and the footwall subject to considerable heave in the cave-exhausted stage.

The empirical support comprises 30 mm of shotcrete in the footwall. The effects of increasing the footwall shotcrete to 150 mm and 300 mm on reinforcement load, shotcrete stress, and tunnel convergence are illustrated respectively in Figures 27 and 28 for the retreat-of-undercut stage. It is evident by comparison with Figure 26 that failure of the anchors and rockbolts is arrested by the increase in thickness of the footwall shotcrete. Side- and hangingwall convergences are also much reduced, and the footwall heave is counteracted by this measure. The extent to which the shotcrete is excessively stressed is, however, greatly increased in all walls.

The distributions in reinforcement load, shotcrete stress, and tunnel convergence for a quadrupling of the footwall anchors are shown in Figure 29 for the retreat-of-undercut stage. It is evident that failure of the anchors and bolts is completely arrested by the substantial increase in the footwall anchors. It can be seen from a comparison of Figures 26 and 29 that the shotcrete stresses and tunnel convergences are not significantly affected by this measure.

The empirical support would evidently not be capable on its own to deal with the squeezing conditions induced by

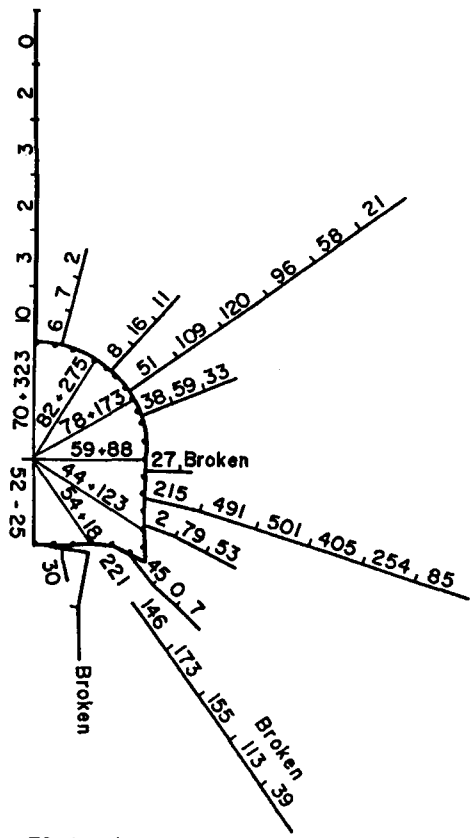

Figure 26—Distribution of reinforcement load for a 4,0 x 4,2 m empirically supported tunnel subject to the retreat-of-undercut stage

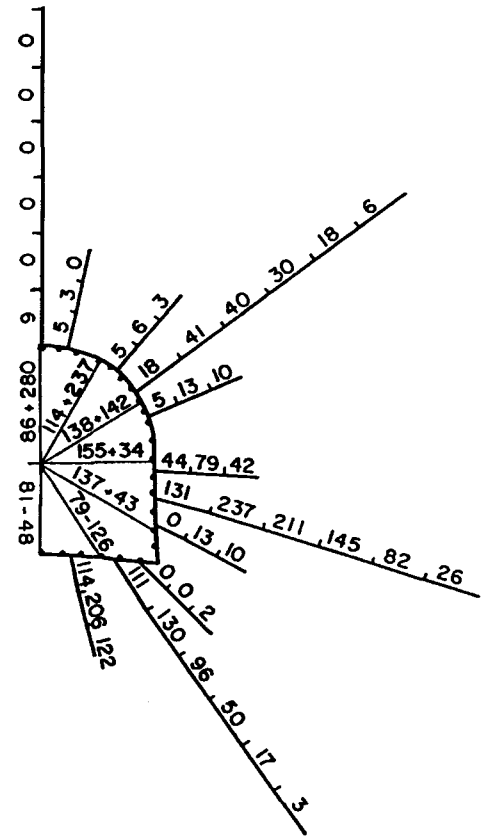

Figure 27—Distribution of reinforcement load, shotcrete stress, and convergence for a 4,0 x 4,2 m empirically supported tunnel, with 150 mm of footwall shotcrete, subject to the retreat-of-undercut stage

the retreat-of-undercut and cave-exhausted loading stages.

Performance of Support Installed

The tunnels in the BA5 block were 4,0 m high x 4,2 m wide and were supported with 1,8 m long fully grouted 12 T rockbolts on a 1,0 m square grid in all walls, 6,0 m long fully grouted 25 T cable anchors on a 2,0 m square grid in all walls, and 150 mm of mesh-reinforced shotcrete in the side- and hanging-walls. The footwall was provided with a cast concrete slab 0,75 to 1,0 m deep.

The bullnoses and camelbacks were in addition provided with 10 25 T horizontal cable straps 300 mm apart and anchored at alternately staggered distances from the apex of 3,5 m and 4,5 m. An additional layer of mesh-reinforced shotcrete 100 mm thick was applied over the cable straps.

The brows of the drawpoints were anchored from the main tunnels. The anchors were installed over the middle 2,0 m section of the sidewalls of the tunnels and effectively covered the entire distance between the bullnoses and camelbacks. The anchors varied in inclination from horizontal to 15 degrees up of horizontal, and in effect doubled the reinforcement of the sidewalls.

The support in the sidewalls was equivalent to the basic support with 150 mm of stress-relieved shotcrete as given for case 14 in Table I. That provided in the hanging- and footwalls was essentially equivalent to the empirical support represented by case 1 in Table I. The shotcrete was not actually stress relieved. It was expected to be damaged and accordingly to be self stress relieving under load.

A number of pillars were provided with five-point sonic probe extensometers and vibrating wire stress meters, which enabled the vertical stress in the centre of the pillars and the displacement of the sidewalls of the crosscut tunnels relative to the centre of the pillars to be monitored. The stresses in the pillars in tuffisitic kimberlite varied from 3 to 7 MPa and in pillars in hypabbysal kimberlite from 25 to 65 MPa for the retreat-of-undercut stage. It can be assumed that the stresses in the pillars were raised by a factor of 2,0. Accounting for the stress-raising effect, the stresses measured in the tuffisitic kimberlite were therefore considerably smaller than the vertical field stress of 34,5 MPa allowed for in the retreat-of-undercut stage in the numerical simulations, and those in the hypabbysal kimberlite approximately equal to that considered in the design at the maxima observed.

The sidewall convergences measured in the tuffisitic kimberlite varied from 20 to 30 mm and in the hypabbysal kimberlite from 5 to 15 mm, compared with corresponding calculated convergences of 40 mm and 20 mm respectively. Although not presented here, sidewall convergence in the hypabbysal kimberlite was simulated similarly to that described for tuffisitic kimberlite. The observed convergences were therefore significantly smaller than predicted by simulation.

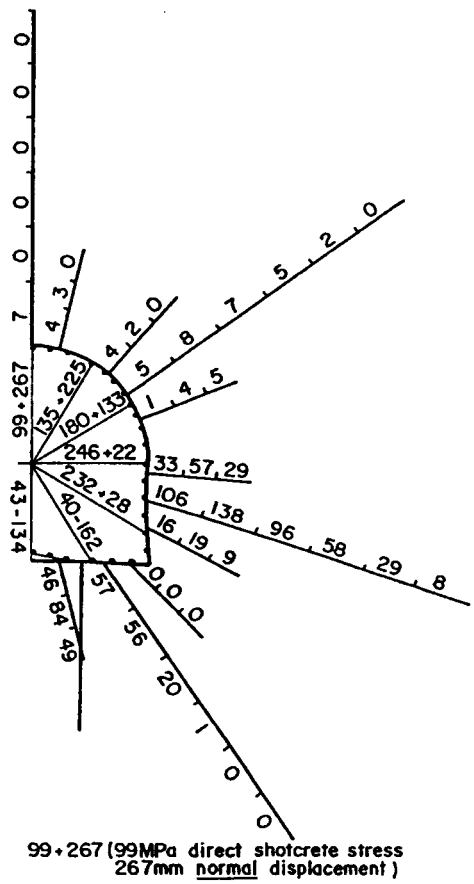

Figure 28—Distribution of reinforcement load, shotcrete stress, and convergence for a 4,0 x 4,2 m empirically supported tunnel, with 300 mm of footwall shotcrete, subject to the retreat-of-undercut stage

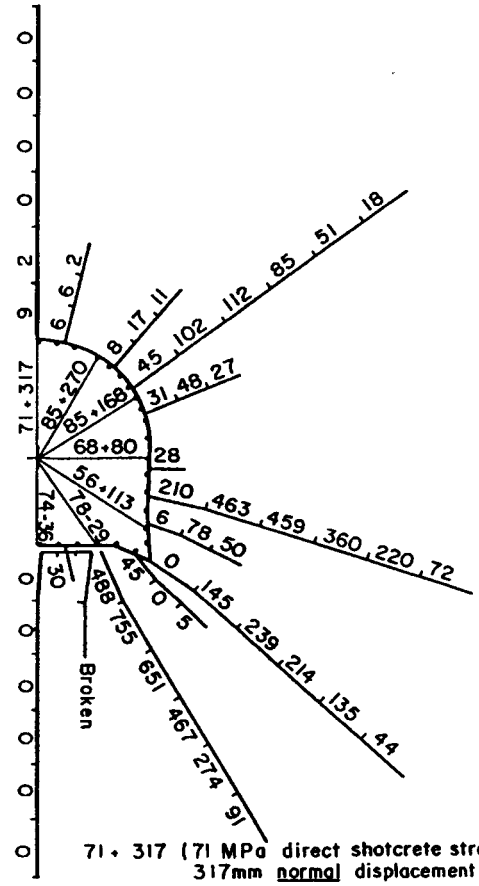

Figure 29—Distribution of reinforcement load, shotcrete stress, and convergence for a 4,0 x 4,2 m empirically supported tunnel, with footwall reinforcement quadrupled, subject to the retreat-of-undercut stage

None of the bolts or anchors installed was observed to have failed during the retreat-of-undercut stage. Cracks were observed in the shotcrete in the sidewalls. These were 5 mm wide at maximum, extended horizontally along the length of the tunnels, and were generally located at a height of about 3,0 to 3,5 m. The cracks did not re-appear after being repaired. In a number of places over which the undercut abutment remained stationary for a period of time, the shotcrete was extensively cracked and spalled. In these instances, sidewall convergence well exceeded 30 mm and corresponded by and large to the calculated displacements. None of the 55 commissioned drawpoints had been lost as a result of support failure when 30 per cent of the planned yield of ore had been abstracted.

The support installed in the main tunnels, crosscuts, and drawpoints evidently proved to be effective during the retreat-of-undercut stage. The underlying design procedures that were developed for the associated demanding squeezing conditions have likewise been shown to be appropriate. Final evaluation of the support effectiveness will, however, be possible only when the block has been mined to completion. The long-recognized understanding that undercut abutments should not be allowed to remain stationary for any length of time has also been confirmed.

SUMMARY

The conclusions can be summarized as follows in terms of rigorously determined support characteristics and a rigorous support-design procedure.

Rigorously Determined Support Characteristics

Relative Stiffness of Shotcrete

- Due to its avidity for load, shotcrete does not function jointly with rock reinforcement. Under conditions of extreme convergence, the shotcrete attracts so much load that it destructs itself.
- Increases in curvature and modulus increase the stiffness of shotcrete and, consequently, its avidity for load.
- The relative stiffness of shotcrete increases at a relatively reducing rate with an increase in thickness. Characteristic minimum shotcrete stresses or thicknesses can, as a result, be found for a particular field-stress situation. This permits determination of whether the minimum shotcrete stress is practically feasible, and whether the corresponding thickness is economically desirable.
- The minimum shotcrete stresses for the field stresses analysed are generally acceptable, but the corresponding thicknesses are far too great for practical purposes.

Support Role of Shotcrete

- If the resulting design thickness for shotcrete as monolithic component is too large for practical purposes, its thickness as surface support between

adjoining elements of rock reinforcement should be determined by simulating it on the basis of multiple stress relief.

Redistribution of Anchor Loads by Shotcrete

- Despite its secondary support role, reinforced multiple stress-relieved shotcrete substantially reduces the anchor loads in the sidewalls, and results in a more uniform distribution in anchor load around the tunnel.

Field Stresses Governing Support Design

- Changes in field stresses displace the ends of the reinforcement relative to one another and, as a result, influence the loads in the reinforcement. Increments in field stresses at the undercut level reduce the reinforcement loads in the hangingwalls of the production tunnels, and increase those in the footwalls. Reductions in the field stresses at the undercut level increase the reinforcement loads in both the hanging- and the footwalls of the production tunnels.
- The retreat-of-undercut and cave-exhausted stages give rise to the largest support loads.

Variation in Anchor Load

- The reinforcement loads are the largest in the sidewalls of the production tunnels for these two loading stages.

Tunnel Shape and Size

- Increases in tunnel dimensions are accompanied by increases in reinforcement load. The increase in reinforcement load in the sidewall due to an increase in tunnel height is considerably larger than the increase in reinforcement load in the hanging- and footwalls due to an increase in tunnel width.
- The anchor loads are prohibitively large for the larger sizes of tunnel.
- The actual size of tunnel for which the anchor loads become prohibitively large depends on the strength of the rockmass.
- Relative normal convergences are not significantly changed by changes in tunnel dimensions.
- The relative normal convergences in unsupported tunnels are very sensitive to tunnel dimensions, more so with regard to height than width, and far more so for larger than smaller tunnels.

Footwall Reinforcement

- The omission of footwall reinforcement does not significantly affect the reinforcement loads or the convergences in other walls of the tunnel. The relatively independent behaviour of the walls of a tunnel derives from an unlimited provision of reinforcement capacity. Only when the reinforcement in any one wall is deficient does it become sensitive to that in other walls.
- If unsupported, the footwall may result in being continuously shaved or sliped to such an extent that the support in the sidewalls becomes undermined. If such a situation is likely to arise, the footwall support should not be omitted in the first instance.

Relative Depth of Anchors

- Displacement and end anchor force decrease with increasing anchor depth, but not at significantly reducing rates.
- The maximum anchor force increases with an increase in anchor length.
- The steel–grout bond strength is the criterion that determines anchor depth for the larger tunnels, and anchor efficiency in terms of the product force x length is the criterion for the smaller tunnels.
- A relative anchor depth of 1,37 satisfies the bond-strength requirements in larger tunnels. The shortest length of anchor can be adopted as the most efficient in smaller tunnels, displacements permitting.

Modulus of Anchors/Glass-fibre Anchors

- The maximum loads in glass-fibre anchors are about 70 per cent of those in steel anchors.
- The loads in the rockbolts used with glass-fibre anchors are generally 10 per cent larger than those in the rockbolts used with steel anchors.
- The relative displacements for glass-fibre anchored tunnels are 5 to 10 per cent larger than for steel-anchored tunnels.
- The same criteria determining depth apply to glass-fibre anchors as to steel anchors.
- A relative depth for glass-fibre anchors of 1,57 satisfies the bond-strength requirement in larger tunnels.
- Slightly longer, but considerably lighter, glass-fibre anchors than steel anchors are required in larger tunnels.
- Overall, glass fibre is about 25 per cent more efficient than steel in terms of the product force x length.

Feasibility of Large Tunnels

- The joint benefits of glass-fibre anchors and multiple stress-relieved mesh-reinforced shotcrete enable larger sizes of tunnel to be considered than is possible with steel anchors.

Strength and Efficiency of Grouting of Reinforcement

- The magnitude and distribution of anchor force are related to bond strength up to 1250 kN/m, at which value the distribution is very uneven. The required capacity for the anchors can be kept relatively small and uniform around the excavation if the bond strength is limited to 1000 kN/m.
- Such marginal constraint on bond strength results in some anchors in the sidewall becoming debonded but, because of the effective splicing effect between adjoining overlapping bolts and anchors, without adversely affecting displacements.
- In the absence of end anchorages and face plates, grouting of only either the back or front halves of the anchors gives rise to significant increases in tunnel displacement and great reductions in anchor forces.
- With the provision of end anchorages and face plates, the only effect of partially grouting either the front or back sections of the anchors is to reduce the forces in the back sections to magnitudes comparable with that when the anchors are fully grouted. In the absence of any grout, the anchor forces are twice as large as when fully grouted.

Rockmass Strength

- An increase in rockmass cohesion from 0,5 to 1,5 MPa is accompanied by an average reduction of 60 per cent in the reinforcement loads.

Appraisal of Empirically Determined Support

- Classification systems provide for two aspects:

quantification of rockmass properties, and design of structural components.
- Such systems lack refinement and rigour with regard to the design aspect, but could be very useful in the determination of the rockmass parameters required in rigorous numerical analyses.

Rigorous Support-design Procedure

The support characteristics described above form the basis of a systematic design procedure, which can be summarized as follows.
- The minimum characteristic stress and thickness for intact shotcrete applicable to a particular rockmass condition and field-stress state can be established by simulation as a first step.
- If neither the stress nor the thickness so determined is acceptable, the shotcrete can be simulated in the subsequent design process as a stress-relieved medium by the introduction of appropriately located gaps in it.
- Both the short and the deeply penetrating rock reinforcement can be spaced on 1,0 m square grids in the subsequent design simulations and should not be limited in load capacity. This would allow the distribution in reinforcement demand around the excavation to develop freely.
- The capacity of the rock reinforcement can then be appropriately sized from the calculated distribution in demand.
- Relative depths of 1,37 and 1,57 can be assumed for steel and glass-fibre anchors respectively for the larger tunnels. The shortest anchors can be adopted for smaller tunnels, displacements permitting.
- The thickness and reinforcement content of the shotcrete can be determined from the calculated bending stresses to which it may be subjected as a thrust-relieved medium.
- If the resulting thickness and reinforcement content of the shotcrete are not practically feasible, diamond mesh suspended in catenary can be designed as surface support between adjoining elements of rock reinforcement.
- The development support comprises 20 T x 1,8 m long fully grouted rockbolts. If used to secure the surface support, both the capacity and the depth of the development support should be determined by rigorous analysis. The surface support can alternatively be secured by cable anchors.

ACKNOWLEDGEMENTS

The permission of De Beers Consolidated Limited, Premier Mine Division, to publish this paper is gratefully acknowledged. The assistance provided by Mr Colin Speers of Steffen Robertson & Kirsten in carrying out the various computer analyses and reducing the results is very much appreciated.

REFERENCES

1. ROSE, D. Steel fibre reinforced shotcrete for tunnel lining: The state of the art. *Proceedings of the Rapid Excavation and Tunnelling Conference*, 1985. vol. 1, pp. 392-412.
2. KIRSTEN, H.A.D. The combined Q/NATM system—The design and specification of primary tunnel support. *S. Afr. Tunnelling*, vol. 6, no. 1. 1986. pp. 18-24.
3. CUNDALL, P.A. Explicit finite difference methods in geomechanics. *Proceedings EF Conference on Numerical Methods in Geomechanics*. Blacksburg, Virginia, 1976. pp. 132-150.
4. KNIGHT, P.S. Geology of the BA5 block cave area of Premier Mine: Its structural stability and support requirements. M.Sc. thesis, Camboume School of Mines, Cornwall, 1988.
5. ESTERHUIZEN, G.S. Stress analyses to evaluate extraction level layouts for the BA5 block cave. Report, Department of Mining Engineering, University of Pretoria, 1986.
6. KIRSTEN, H.A.D., STACEY, T.R., and MCCRACKEN, A. Premier Mine—tunnels and orepass stability. Steffen Robertson & Kirsten report, no. CI 5928/2, 1988.
7. KIRSTEN, H.A.D. Norwegian Geotechnical Institute or Q System by N. Barton. Discussion contribution. *Symposium on Rock Classification Systems for Engineering Purposes*, D-18, ASTM STP 984, ASTM, Cincinnati, 1988. pp. 85-88.
8. DIERING, J.A.C. Mining simulation of tabular excavations using finite elements. *Proceedings of the Fourth International Conference on Numerical Methods in Geomechanics*. Edmonton, 1982. vol. 2, pp. 545-550.
9. KIRSTEN, H.A.D. Comparative efficiency and ultimate strength of mesh- and fibre-reinforced shotcrete determined from full-scale bending tests. J. S. Afr. Inst. Min. Metall.

ADDENDUM 1
DEFINITION OF SYMBOLS AND ABBREVIATIONS

The following symbols and abbreviations are used in this paper.

FLAC	Fast Lagrangian analysis of continua
Q	Barton *et al.*'s rockmass classification index $= (RQD \cdot J_r \cdot J_w)/(J_n \cdot J_a \cdot SRF)$
NATM	New Austrian Tunnelling Method
Q-NATM	Empirical support-design system based on Q index and NATM
RQD	Designation of rock quality
J_n	Joint-set number
J_r	Joint-roughness number
J_a	Joint-alteration number
J_w	Joint-water number
SRF	Stress reduction factor
E	Young's modulus
μ	Poisson's ratio
UCS	Uniaxial compressive strength = $2 \cdot c \cdot \cos \Phi/(1 - \sin\Phi)$
c	Cohesion
ϕ	Friction angle
u	Subscript designating intact rock
m	Subscript designating rockmass

ADDENDUM 2
MATERIAL PROPERTIES

Laboratory Test Results and Classification Parameters

The densities for the intact and *in situ* rock given in Table II were arbitrarily taken as 2,65.

The *RQD* for intact rock is by definition 100 per cent, and that for *in situ* rock is determined from field mapping. The Young's moduli, Poisson's ratios, and uniaxial

compressive and tensile strengths given in the table for intact rock were determined from small-scale laboratory tests. The friction angles for the intact and *in situ* rock were arbitrarily assumed as shown in the table.

The Young's modulus for the *in situ* rock was determined from a curve fitted to the plot in Figure A1 of the ratio of Young's moduli for *in situ* and intact rock, E_m/E_u, against the rock-quality designation for *in situ* rock, RQD_m (Deere *et al.*[1]). The expression for the curve can be shown to assume the form

$$\log(E_m/E_u) = 1{,}44 \times RQD_m^2 - 0{,}44 \times RQD_m - 1{,}0. \quad [1]$$

According to Deere and Miller[2], the uniaxial compressive strength and Young's modulus are proportional to each other. The cohesion given in Table II for the *in situ* rock, c_m, was accordingly determined from the following expression in terms of the cohesion for the intact rock, c_u, the ratio of Young's moduli, E_m/E_u, and the friction angles Φ_m and Φ_u:

$$c_m = c_u \times (E_m/E_u) \times \tan(45° - \Phi_m/2)/\tan(45° - \Phi_u/2). \quad [2]$$

Quantitative Evaluation of Field Measurements

The measurements taken with an extensometer in the sidewall of tunnel 109 on level 553 m in Stope SA1, block L1, of the mine are shown in Figure A2. The associated vertical and horizontal field stresses were assumed to be equivalent to heads of rock of 184 and 553 m respectively.

The section shown in Figure A2 was simulated with FLAC as a continuum devoid of joints. Adjoining tunnels and the actual support, which comprised 3 m long untensioned grouted rockbolts on a 1 m square grid in the side- and hangingwalls, were included in the analysis. Young's modulus, Poisson's ratio, and the friction angle

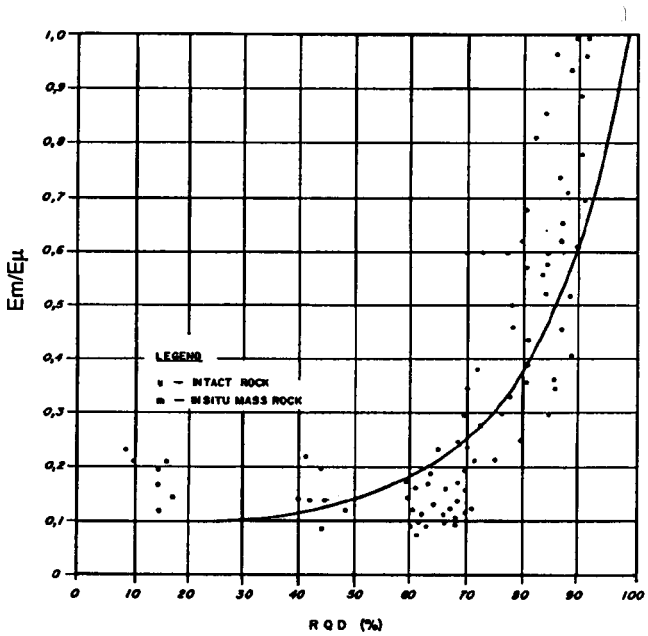

Figure A1—Plot of modular ratio against rock-quality designation

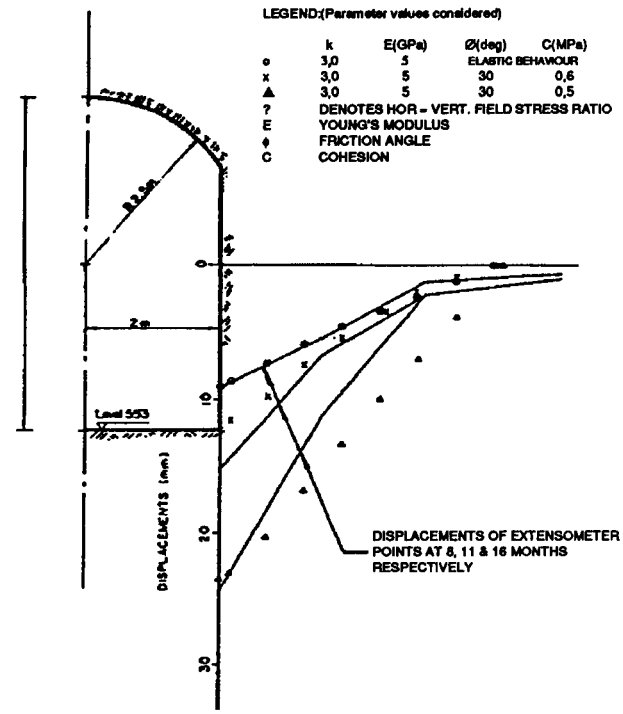

Figure A2—Variation of observed and calculated displacement with depth

were taken as 5 GPa, 0,2, and 30° respectively. Five values were considered for cohesion: 2 MPa, 1 MPa, 0,7 MPa, 0,65 MPa, and 0,5 MPa.

The corresponding calculated distributions of sidewall displacement are superimposed on the field data in Figure A2, from which it can be seen that a cohesion for the rockmass of 0,5 MPa most closely approximates the extensometer readings at 18 months. In the context of geological variability, this value is not significantly different from that given in Table II, 1,1 MPa.

Qualitative Assessment of Field Measurements

The side- and hangingwall displacements of 24 and 11 mm referred to above subsequently increased owing to mining to 120 and 78 mm respectively in about eight months. The on-going nature of the displacements represented a condition of indeterminacy, which enabled a qualitative estimate of the *in situ* mass cohesion to be made as discussed in this paper.

It is evident from Figure 3 of the paper that the cohesion for the rockmass at the onset of indeterminate displacements at a friction angle of 30° is 0,4 MPa. This value corresponds very closely to that back-analysed from the displacement data, 0,5 MPa, and is also not significantly different from the value of 1,1 MPa given in Table II.

REFERENCES

1. DEERE, D.U., HENDRON, A.J., PATTON, F.D., and CORDING, E.J. Design of surface and near-surface construction in rock. *Proceedings Eighth Symposium on Rock Mechanics*. Minnesota, 1966.
2. DEERE, D.U., and MILLER, R.P. Engineering classification and index properties of rock. *Technical Report* No. AFWL-TR-65-116, Air Force Weapons Laboratory, Kirtland Air Force Base, New Mexico, 1966.